Original Research

Proliferation and differentiation of osteoblasts from the mandible of osteoporotic rats

Shu-Juan Yu[1], Hong-Chen Liu[2], Ling-Ling E[2], Dong-Sheng Wang[2] and Guo-Xiong Zhu[1]

[1]Department of Stomatology, The General Hospital of Jinan Military Region of PLA, Jinan 250031; [2]Institute of Stomatology, The General Hospital of PLA, Beijing 100853, China

Corresponding authors: Guo-Xiong Zhu, 25 Shifan Road, Tianqiao District, Jinan 250031, China and Hong-Chen Liu, 28 Fuxing Road, Haidian District, Beijing 100853, China. Emails: zhuguoxiongkq@163.com and liuhongchenkq@163.com

Abstract

The objective of this study was to identify the differences between osteoblasts derived from normal adult rat mandibles and osteoporotic adult rats. An osteoporotic animal model was established by performing a bilateral ovariectomy (ovx group). The proliferation and differentiation abilities of osteoblasts were determined by MTT (3-[4,5-dimethylthiazol-2-yl]-2,5-diphenyl-2*H*-tetrazolium bromide), alkaline phosphatase (ALP) and osteocalcin release (OC) assays. Transmission electron microscopy (TEM) was performed to assess differences in the ultrastructure. Proliferating cell nuclear antigen (PCNA) and uncoupling protein 2 (UCP2) protein concentrations were analyzed by Western blot. In addition, UCP2 protein in osteoblasts was assessed by immunohistochemistry staining. ATP and reactive oxygen species (ROS) concentrations were analyzed separately with ATP and ROS quantification kits. At four and 12 weeks after the operation, osteoblasts of the ovx group showed earlier attachment, fewer dead cells and faster growth compared with cells in the sham group. TEM showed that osteoblasts of the ovx group had fewer folds, lysosomes, peroxisomes and less rough endoplasmic reticulum. The results of the MTT, ALP activity and OC assays were all higher in osteoblasts from the ovx group at four or 12 weeks postsurgery than osteoblasts from the sham group. PCNA protein concentrations in the ovx group increased significantly compared with those of the sham group at four or 12 weeks after the operation, but UCP2 concentrations decreased over the same time period. UCP2 immunohistochemical staining of osteoblasts showed that the protein was concentrated in the cytoplasm and that the osteoblasts from the sham group had higher expression than those from the ovx group. The ATP and ROS concentrations of the ovx groups were significantly higher than the sham groups at four or 12 weeks postsurgery. Therefore, we concluded that there are differences in cell ultrastructure, proliferation, differentiation, ATP and ROS concentrations, and PCNA and UCP2 protein expression levels in osteoblasts from the mandibles of rats of the ovx group compared with those from the sham group.

Keywords: osteoblasts, osteoporosis, jaw

Experimental Biology and Medicine 2012; **237**: 395–406. DOI: 10.1258/ebm.2011.011217

Introduction

Estrogen deficiency typically occurs in women during postmenopause and has been shown to be effective in accelerating the bone re-modeling process, which usually results in higher levels of bone resorption than bone formation (osteoporosis).[1] Osteoporosis is a condition of decreased bone mass and increased susceptibility to fractures, and represents the most common systemic metabolic bone disease.[2] Although the effects of osteoporosis on decreased bone quality and increased risk of fracture of long bones and vertebra are well established, the effects on jaw bone are less understood. Bones of the jaw contain teeth and therefore are arguably more complex than other bones. The functional demands of mastication on alveolar bones increase the complexity of both the structural makeup and subsequent mechanical properties. Interestingly, some reports have shown that osteoporosis is closely related to the loss of jaw bone, periodontal disease, tooth loss and implantation.[3,4]

Osteoporosis is characterized by an imbalance between the activity of osteoblasts, which are the bone-forming cells, and the osteoclasts, which are the cells that resorb the bone tissue.[5] Osteoporosis is regulated by controlling the number and activity of osteoblasts, so in order to fully understand this process, it is necessary to study changes

in cell function and microstructure. Mitochondria are the fundamental organelles of cellular energy metabolism. The changes in mitochondrial function and number play important roles in proliferation and differentiation of osteoblasts.[6,7] It has been shown that over 90% of oxygen molecules are consumed by mitochondria *in vivo*, which generates ATP to meet energy needs of the body, as well as used as reactive oxygen species (ROS). Although ATP secretion has been well characterized with regards to osteoblast proliferation,[8] little is known about the molecular mechanisms of ATP regulation in osteoblasts under osteoporotic conditions. Epidemiological evidence in humans and recent mechanistic studies in rodents have indicated that ROS greatly influence the generation and survival of osteoblasts. Moreover, recent data have shown that ROS, such as H_2O_2-generated superoxide anions, are able to influence osteoblastic differentiation.[9] The uncoupling protein 2 (UCP2) was discovered in 1997 on the mitochondrial membrane and is widely distributed in a variety of tissues and organs of humans and rodents. As a proton transport protein, UCP2 allows protons to directly enter the mitochondrial matrix without involvement in ATP synthesis.[10] This process also reduces ROS production due to the reduction of the proton gradient and electron leakage.[11] However, the presence of UCP2 in the bone or osteoblasts has not been reported, and no study to date has examined the roles of UCP2, ATP and ROS together in osteoporosis.

The study of osteoblasts *in vitro* eliminates a number of influential factors that are present *in vivo*, and therefore this method can provide very valuable experimental data for bone metabolism. However, several previous studies of osteoporotic mechanisms were restricted to normal bone cells from the calvarial or femur bones.[12,13] Due to the unique anatomy, location and function of the mandible, characterizing osteoblasts that are derived from the osteoporotic mandible may provide an important study approach for osteoporotic jaws. Therefore, this study compared osteoblasts obtained from the mandibles of osteoporotic rats with osteoblasts obtained from the mandibles of normal rats in order to assess proliferation, differentiation and related protein expression. We also established an *in vitro* method for culturing mandible osteoblasts isolated from osteoporotic rats, which represent cells that are potentially the origin for osteoporosis in the jaw and an important focus of oral medicine.

Materials and methods

Establishment of the animal model

All animal experiments were approved by our Institutional Animal Care and Use Committee. Twenty-three-month-old female Sprague–Dawley (SD) rats (Experimental Animal Center of Military Medical Sciences, Beijing, China) weighing approximately 300 g were randomly divided into two equal groups. Group 1 served as a control (sham), and a small piece of fatty tissue near the ovary was removed from the rats of this group. For Group 2, we performed bilateral ovariectomy on the rats, which served as an osteoporotic animal model based on a previously established method.

Measurement of bone mineral density and serum estradiol concentrations

SD rats were anesthetized with 1% pentobarbital and measured with a DEXA scanner (GE Lunar Prodigy, GE Healthcare, Madison, WI, USA). To measure the lumbar spine and femoral bone mineral density (BMD), the rats were placed in the prone position on the DEXA plate and the X-ray tube was aligned along the longitudinal axis at the midpoint of the body. The mandibular BMD was measured when the rats were in the lateral position. The BMD value was determined using small animal analysis software (Prodigy enCORE software version 10.50.086, GE Lunar Prodigy; GE Healthcare). The coefficient of variation for the BMD of the lumbar spine, femoral and mandible was 0.83, 0.65 and 1.27%, respectively.

Retinal artery blood from rats was incubated at room temperature for 30 min and then centrifuged at 3000 rpm for 10 min. The upper serum was then removed and stored at -80°C for future measurement. Estradiol (E_2) concentrations in the serum were measured using an estradiol radioimmunoassay kit (North Bio Tech, Beijing, China).

Hematoxylin and eosin staining of mandibular bone

Mandibular tissue specimens from SD rats at four and 12 weeks after the operation were fixed with 10% formaldehyde, decalcified with 10% ethylenediaminetetraacetic acid, dehydrated with graded alcohol and embedded in paraffin. The specimens were serially cut into 5 μm thick sections in the mesial and distal direction of the teeth and then stained with hematoxylin and eosin (H&E). The sections were observed under an optical microscope.

Osteoblast isolation, culture and expansion in medium

At four, 12 and 20 weeks after the operation, the rats from the two groups were euthanized under general anesthesia and soaked in 75% ethanol for five minutes. The mandibles of the rats were then removed under sterile conditions, rinsed in 75% ethanol for 5–10 s, immersed in 5.25% NaClO for one minute and washed three times with phosphate-buffered saline (PBS). The muscles and fascia were then completely stripped and the teeth were removed. The mandible was cut into 2 mm $\times$ 2 mm bone slices and the bone slices were washed with PBS to remove residual blood. Osteoblasts were isolated by incubation with trypsin.

Alkaline phosphatase staining

Osteoblasts were seeded on coverslips at an inoculation density of 1×10^4 cells/mL in six-well plates and fixed with 95% ethanol for 10 min after culturing the cells for 24 h in order to make cell-climbing slices. The coverslips were incubated with a solution containing 5 mL 2% pentobarbital sodium, 5 mL 3% β-glycerophosphate, 10 mL 2% calcium nitrate, 5 mL 2% magnesium sulfate and 25 mL distilled water for four hours at 37°C. The coverslips were then washed with distilled water and placed in a solution of 2% calcium nitrate and cobalt nitrate for two minutes. They

were then washed with distilled water and placed in 1% ammonium sulfate for one minute. Finally, the slices were completely washed with tap water, dehydrated with alcohol, made transparent with xylene and sealed with resin.

Alizarin red S staining of calcium tubercles

Osteoblasts were seeded on coverslips at an inoculation density of 1×10^5 cells/mL in six-well plates and fixed with 95% ethanol for 10 min after culturing the cells for 24 d in order to make cell-climbing slices. The slices were then rinsed with PBS and fixed with acetone. Calcium tubercles were stained for one minute with 20 μL of 1% Alizarin red S and washed twice with 1 mL of distilled water per wash. Calcium tubercles were then observed and identified by light microscopy.

Collagen I staining of osteoblasts

Osteoblasts were seeded on coverslips and cultured. The cells were then fixed with 95% ethanol and washed with PBS. One drop of iron hematoxylin was placed on the coverslips for five minutes and the coverslips were washed with PBS three times. The coverslips were washed with tap water for 10 min and dyed by incubation with picric acid fuchsin for five minutes. After rapid differentiation with 95% ethanol and treatment with xylene to make the cells transparent, the coverslips were observed under an inverted microscope.

3-(4,5-dimethylthiazol-2-yl)-2,5-diphenyl-2*H*-tetrazolium bromide assay

Cell proliferation was determined by the MTT (3-[4,5-dimethylthiazol-2-yl]-2,5-diphenyl-2*H*-tetrazolium bromide) assay. Briefly, osteoblasts from the ovx and sham groups at four and 12 weeks postsurgery were inoculated in a 96-well plate (1×10^4 cells/well; 200 μL per well) and grown for 72 h at 5% CO_2 and 37°C. The MTT solution (20 μL) was added in each well and incubated at 37°C for four hours. After the formation of formazan crystals, MTT medium was aspirated and replaced with dimethyl sulfoxide to dissolve the formazan crystals. The plates were read on an enzyme-linked immunosorbent detector (ELx800 UV-type; Bio-Tek, Winooski, VT, USA) at a wavelength of 490 nm.

Intracellular and media activity of alkaline phoshatase and protein assay

Fourth generation osteoblasts from the ovx and sham groups at four and 12 weeks postsurgery were seeded in six wells each of a 12-well plate (1×10^5 cells/well; 1 mL per well) and grown for three days at 5% CO_2 and 37°C. The cells were then washed with PBS and lysed in 300 μL of 0.1% Triton X-100 overnight at 4°C. The lysates (50 μL) were transferred to another 96-well plate and 50 μL of 4.5 mmol/L para-nitrophenylphosphate was added. The plate was then incubated at 37°C for an additional 30 min. To terminate the reaction, 50 μL of 0.1 mol/L NaOH was added to each well. The optical density for the enzyme products was measured at a wavelength of 405 nm. A protein assay (Bicinchoninic acid [BCA] Protein Assay Kit; Boster, Wuhan, China) was used to normalize protein.

Osteocalcin assay

Osteoblasts were seeded in a 12-well plate (1×10^5 cells/well; 1 mL per well) and cultured for three days. The cell culture medium was then collected and the content in the culture medium was detected using an automatic electrochemiluminescence immunoassay (Cobas E601; Roche, Basel, Switzerland).

Transmission electron microscopy of osteoblasts

Osteoblasts from the ovx group at 12 weeks postsurgery were collected, re-suspended at a concentration of 2×10^7 cells/mL and washed with PBS (pH 7.4) two times. The osteoblasts were then centrifuged for five minutes at 1500 rpm. The cell mass was fixed with 1.5% glutaraldehyde for four hours followed by incubation in 1% oxide osmium for one hour. After the cell mass was dehydrated with an acetone gradient, the cell mass was impregnated and embedded in epoxy resin, sliced to a 50 nm thickness and double-stained with uranyl acetate and lead citrate. The osteoblasts were then observed by transmission electron microscopy TEM (JEM 100CX-II; JEOL, Tokyo, Japan).

UCP2 immunohistochemistry

Osteoblasts from the sham and ovx groups were seeded on slides (2.4 cm × 2.4 cm) at 1×10^5 cells/mL. After 24 h, the slides were fixed with 95% ethanol and detected using the Strept-Avidin-Biotin Complex (SABC) immunohistochemistry method (Boster). Briefly, the slides were washed with PBS (5 min × 3 times), incubated with 0.1% TritonX-100 for 20 min at room temperature and washed again with PBS (5 min × 3 times). A 5% BSA blocking solution was then incubated with the slides for 20 min at room temperature. The excess liquid was removed and the appropriate primary antibody (diluted 1:100; Boster) was incubated with the slides overnight at 4°C. The next day, the slides were washed with PBS (5 min × 3 times), incubated with secondary antibody (Boster) for 60 min and washed with PBS again. The SABC reagents were then added and the slides were incubated for an additional 20 min at 37°C. After the incubation, the slides were washed four times with PBS (5 min for each wash). The slides were then colored with a mixture of reagents A, B and C from the 3, 3′-diaminobenzidine tetrahydrochloride (DAB) color kit (Boster) together with 1 mL distilled water. The reaction time was controlled by observation under the microscope. Distilled water was used to wash the slides and stop the reaction. Finally, the slides were dehydrated, made transparent and mounted.

Western blot

Osteoblasts were washed with PBS three times and directly lysed. The plate was gently shaken for 15 min on ice. The osteoblasts in each well of the plate were scraped with a cell

scraper, collected in 1.5 mL Eppendorf tubes and centrifuged at 12,000 *g* for 15 min at 4°C. The supernatants were normalized to contain equal amounts of protein (30 μg), separated by 8% sodium dodecyl sulfate polyacrylamide gel electrophoresis and electro-transferred to 0.45 μm polyvinylidene difluoride membranes (Millipore, Bedford, MA, USA). Following the transfer, the membranes were blocked with a solution of 0.1% Tris-buffered saline-Tween (TBS-T) wash buffer (containing 5% non-fat milk, pH 7.4) overnight at 4°C and then incubated with primary antibody (rabbit anti-rat UCP2, final dilution 1:300; mouse anti-rat proliferating cell nuclear antigen [PCNA], final dilution 1:400; anti-β-actin, final dilution 1:2000; Boster) for two hours at 37°C. The membranes were then washed with TBS-T solution (10 min × 3 times) and horseradish peroxidase-labeled goat anti-rabbit IgG and goat anti-mouse IgG were added (final dilution 1:2000) and incubated for one hour at 37°C. After the secondary incubation, the membranes were washed with TBS-T (10 min × 3 times) and the membranes were placed in chemiluminescence substrate and incubated for five minutes at room temperature with rapid shaking. The membranes were subsequently exposed for two minutes to film.

For analysis, the blots were scanned and quantified using Quantity One analysis software (Bio-Rad, Hercules, CA, USA). The results were expressed as a percentage of β-actin immunoreactivity.

ATP quantification

ATP concentrations in osteoblasts were measured with the ATP assay kit (Beyotime, Nantong, China) according to the manufacturer's instructions. Briefly, osteoblasts were seeded in six-well plates at 3×10^5 cells/mL and cultured for 24 h to reach 80% confluence. The osteoblasts were lysed in the same plate for 10 min using the reagent provided in the kit. After lysis, the mixtures were centrifuged at 12,000 *g* for 10 min at 4°C while the ATP detection working solution was incubated in opaque-walled, 96-well plates for five minutes to reduce the background of ATP. The supernatant of the samples was then transferred into opaque-walled, 96-well plates for two seconds and luminescence was immediately measured with a versatile fluorescent light analyzer (FLUOstar Omega; BMG Labtech, Offenburg, Germany) at a 562 nm wavelength. The ATP concentration was calculated based on a standard curve generated from the ATP standard solution that was provided with the ATP assay kit. Protein content was measured with the BCA protein assay kit (Beyotime).

Osteoblast ROS quantification

Intracellular ROS concentrations were analyzed with the Reactive Oxygen Species assay kit (Beyotime) using 2′,7′-dichlorodihydrofluorescin diacetate (DCFH-DA). Briefly, osteoblasts were seeded in six-well plates at a density of 1×10^6 cells/mL and cultured for 24 h to reach 80% confluence. The cells were then washed twice with PBS and the DCFH-DA probe diluted with serum-free culture medium (1:1000 dilution) was added to the plates. The osteoblasts were incubated for an additional 20 min at 37°C with 5% CO_2. Each well was washed with serum-free cell culture medium three times to fully remove the remaining DCFH-DA, placed in centrifuge tubes and centrifuged at 800 rpm for six minutes. The cells were washed with PBS and re-suspended in 0.3 mL PBS. From this suspension, 0.2 mL of solution containing cells was transferred to a 96-well plate and the fluorescence was measured with a versatile fluorescent light analyzer (FLUOstar Omega; BMG Labtech) at an excitation/emission wavelength of 488/525 nm. The mean fluorescence values of DCFH-DA-loaded cells were corrected by subtracting the autofluorescence background.

Statistical analysis

The results were expressed as mean ± standard deviation. Statistical analysis was performed by analysis of variance, followed by adequate subtests when statistical significance was reached. A P value equal to or less than 0.05 was considered significant.

Results

The establishment of osteoporosis in a rat model

We first compared the BMD and serum estradiol concentrations of rats in the sham and ovx groups and found that the BMD of the lumbar spine and femur from rats of the ovx group decreased significantly ($P < 0.05$) compared with the sham group 12 weeks after the operation (Table 1). These results suggested that the rats from the ovx group were osteoporotic at 12 weeks postsurgery. In addition, there was a decreasing trend in BMD of the rat mandibles in the ovx group 12 weeks after the operation, but the results were not significant ($P > 0.05$). There were no significant differences in estradiol concentrations between the sham and ovx groups before the operation. At the same time point after surgery, serum estradiol concentrations of rats in the ovx group were significantly lower than the sham group ($P < 0.05$), indicating that we successfully established a rat model of osteoporosis.

H&E staining of tissue sections

H&E staining of tissue around the apical area of teeth at different time points is shown in Figure 1. The apical area of the teeth from rats in the sham group had denser trabecular bone, and the trabecular space was smaller compared with teeth from rats in the ovx group. In addition, the trabecular bone at the apical area in the teeth of rats from the ovx group was reduced, sparsely arranged and the trabecular separation was widened.

Identification and morphology of osteoblasts by microscopy

There was no significant difference in the morphology of osteoblasts between the ovx group and sham group, which exhibited long spindle-like, triangle and polygon morphologies (Figure 2a). However, at four and 12 weeks

Table 1 The BMD of the lumbar spine, femoral and mandibular bones and serum estradiol concentration

Group	BMD (g/cm^2)			E_2 (ng/L)
	Lumbar spine	Femoral	Mandibular	
Sham group (0 weeks)	0.207 ± 0.019	0.261 ± 0.024	0.372 ± 0.024	107.42 ± 12.01
Ovx group (0 weeks)	0.204 ± 0.011	0.267 ± 0.015	0.378 ± 0.033	110.23 ± 15.16
Sham group (4 weeks)	0.242 ± 0.015	0.287 ± 0.015*	0.406 ± 0.013*	103.22 ± 11.25
Ovx group (4 weeks)	0.202 ± 0.028*	0.268 ± 0.010*	0.462 ± 0.018*	67.43 ± 9.28
Sham group (12 weeks)	0.245 ± 0.029	0.314 ± 0.017*	0.414 ± 0.036	96.24 ± 12.31
Ovx group (12 weeks)	0.190 ± 0.029*	0.263 ± 0.022	0.393 ± 0.018	45.19 ± 8.02
Sham group (20 weeks)	0.240 ± 0.023	0.296 ± 0.031*	0.394 ± 0.007	89.15 ± 9.76
Ovx group (20 weeks)	0.213 ± 0.039*	0.272 ± 0.016*	0.389 ± 0.007	38.21 ± 7.39

BMD, bone mineral density; E_2, estradiol
*$P < 0.05$ for the ovx and sham groups compared at the same time point; $n = 10$

after the operation, both the primary and subcultures of osteoblasts from the ovx group exhibited earlier attachment, fewer dead cells and faster growth than cells from the sham group. Twenty weeks after the operation, the osteoblasts from both the ovx and sham groups grew slowly, did not passage smoothly and exhibited cell death.

The cells stained well with ALP and showed brown and black granules that clustered in the cytoplasm (Figure 2b). In addition, Alizarin red S staining of the osteoblasts showed the formation of red tubercles (Figure 2c). The collagen I staining showed the deposition of an orange substance in the osteoblasts (Figure 2d).

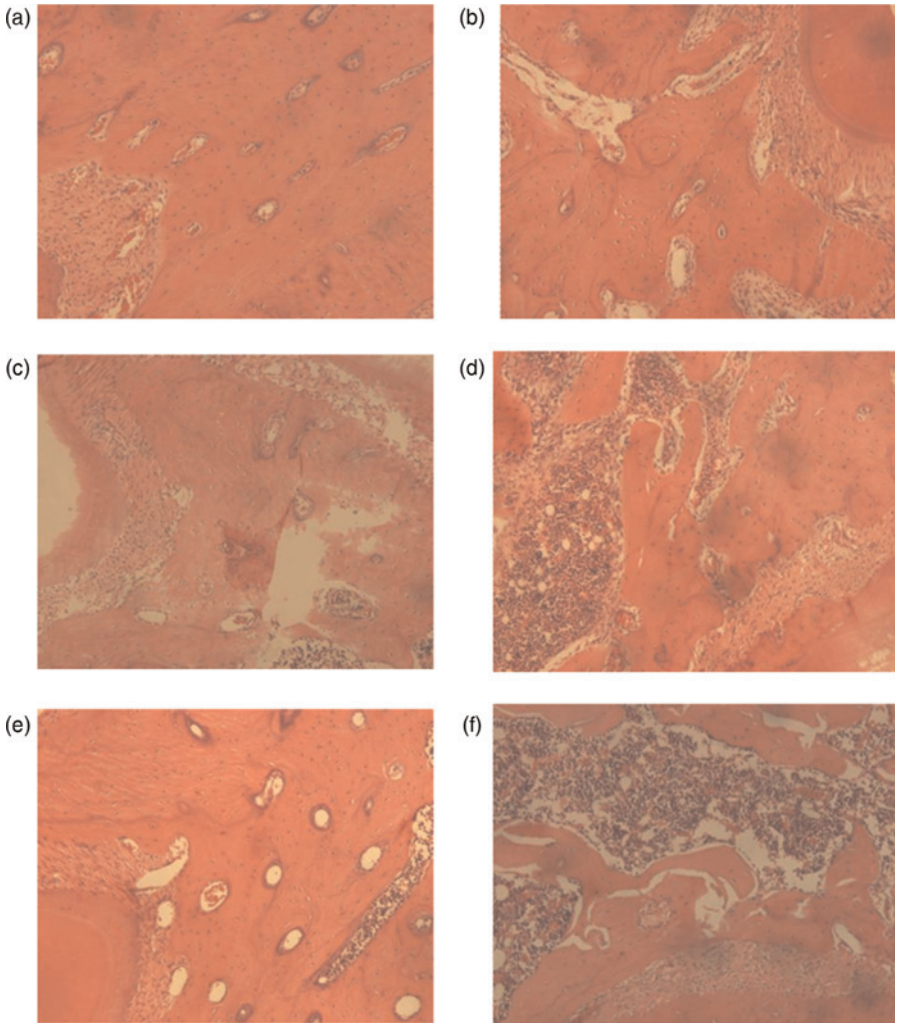

Figure 1 The H&E staining of tissue near the apical area of teeth in the mandible at different time points. (a) H&E staining of mandibular tissue sections from the sham group at four weeks (×100). (b) H&E staining of mandibular tissue sections from the ovx group at four weeks (×100). (c) H&E staining of mandibular tissue sections from the sham group at 12 weeks (×100). (d) H&E staining of mandibular tissue sections from the ovx group at 12 weeks (×100). (e) H&E staining of mandibular tissue sections from the sham group at 20 weeks (×100). (f) H&E staining of mandibular tissue sections from the ovx group at 20 weeks (×100). H&E, hematoxyline and eosin. (A color version of this figure is available in the online journal)

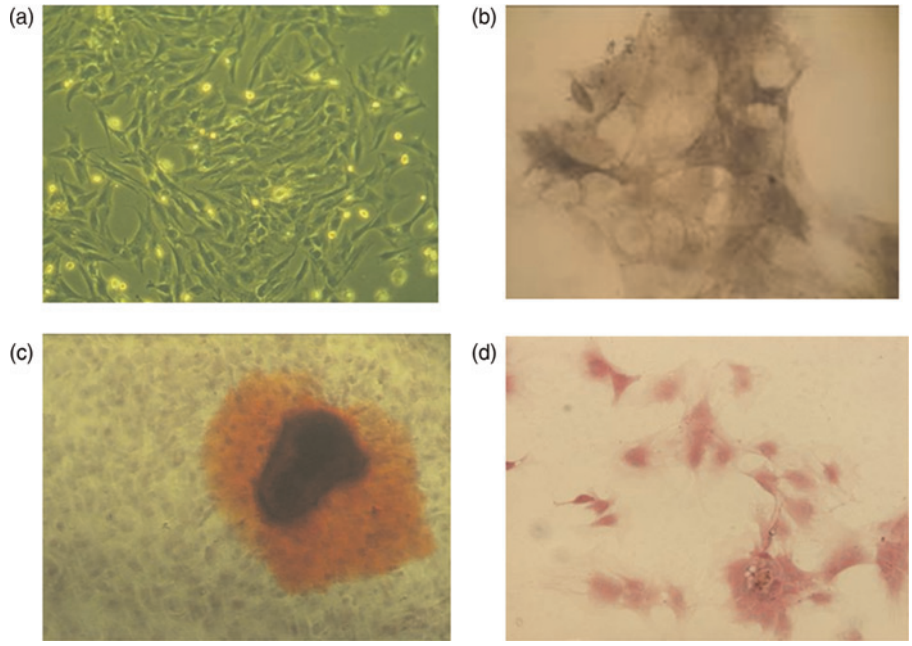

Figure 2 Observation and staining of osteoblasts: (a) osteoblasts from mandibular tissue (×100); (b) alkaline phosphatase staining of osteoblasts (×100); (c) Alizarin red S staining of osteoblasts (100 ×); and (d) collagen I staining of osteoblasts (×100). (A color version of this figure is available in the online journal)

MTT assay of osteoblasts

The proliferation of osteoblasts from the ovx group at four and 12 weeks after the operation was significantly faster than that of the respective rats from the sham group (Figure 3).

ALP activity of osteoblasts

The ALP activity in osteoblasts from the ovx group was significantly higher than that in the sham group four weeks after the operation. Moreover, the difference between the ovx and sham groups was even greater at 12 weeks postsurgery (Figure 4).

Osteocalcin release in cell supernatants

Although the concentration of osteocalcin in the ovx group was higher than in the sham group, the differences at four weeks after the operation were not significant (Figure 5). However, the difference was significant at 12 weeks after the operation.

TEM of osteoblasts

The osteoblasts were mostly flat when observed by TEM (Figure 6). The nuclei of the cells were polygonal in shape, had several folds and contained 0, 1 or 2 nucleoli. The cell surface had many protrusions and microvilli. In addition, the cytoplasm was rich with mitochondria and rough endoplasmic reticulum (Figure 6a). In contrast, the osteoblasts of the ovx group had fewer folds, lysosomes, peroxisomes and less rough endoplasmic reticulum (Figure 6b). Moreover, they had one nucleolus, or in some cases had no nucleoli, and only rarely had two. These cells also contained more heterochromatin and mitochondria than the osteoblasts from the sham group.

PCNA and UCP2 protein expression in osteoblasts

The PCNA protein concentrations in the osteoblasts from the ovx group increased significantly compared with the sham group at four or 12 weeks after the operation (Figure 7). In contrast, the UCP2 protein concentrations in

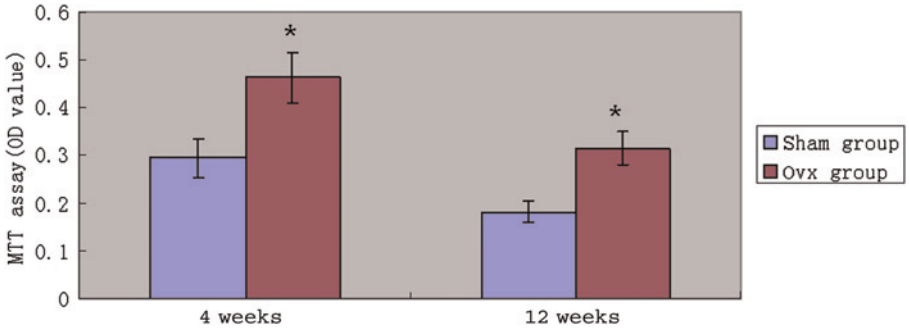

Figure 3 Proliferation analysis of osteoblasts from the ovx and sham groups (*$P < 0.05$ for the ovx and sham groups compared at the same time point). MTT, 3-(4,5-dimethylthiazol-2-yl)-2,5-diphenyl-2*H*-tetrazolium bromide; OD, optical density. (A color version of this figure is available in the online journal)

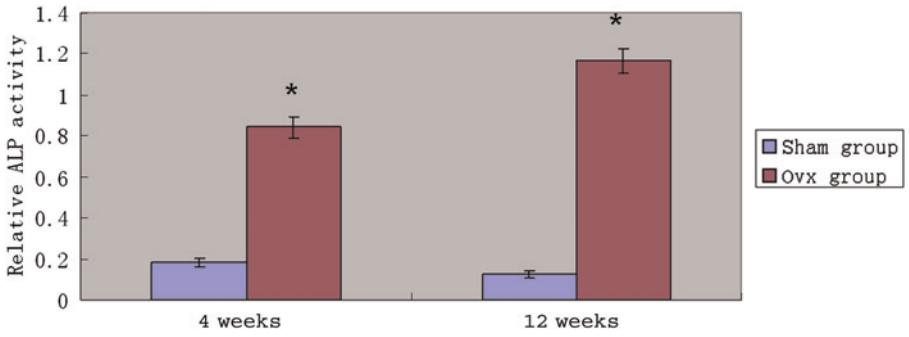

Figure 4 ALP activity of osteoblasts from the ovx and sham groups ($^{*}P < 0.05$ for the ovx and sham groups compared at the same time point). ALP, alkaline phosphatase. (A color version of this figure is available in the online journal)

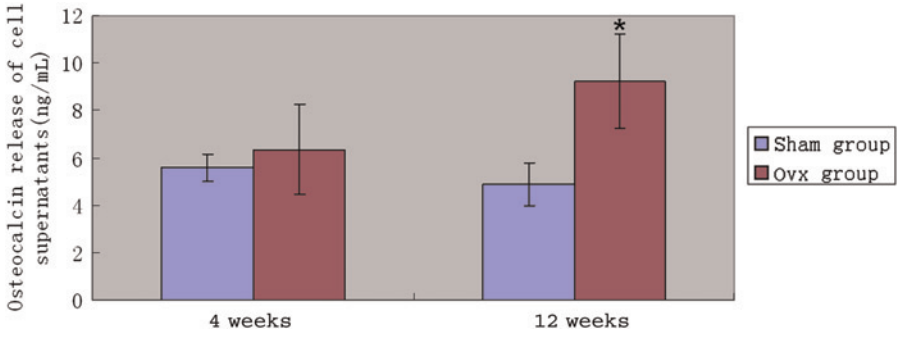

Figure 5 A comparison of osteocalcin release in cell supernatants between the ovx and sham groups at the same time point. $^{*}P < 0.05$. (A color version of this figure is available in the online journal)

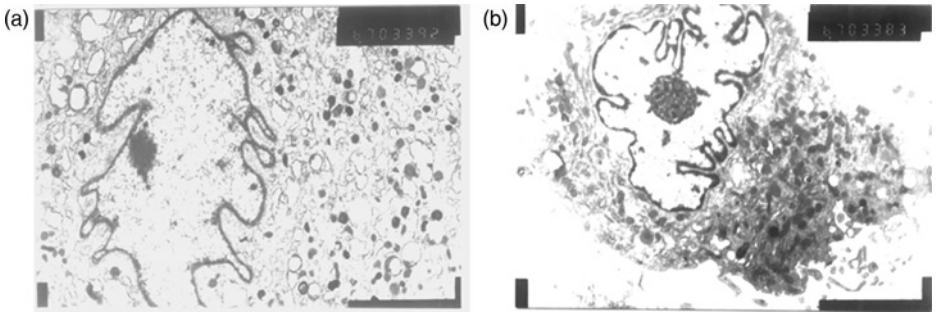

Figure 6 TEM of osteoblasts from the sham and ovx groups: (a) TEM of osteoblasts from the sham group (×6700 magnification) and (b) TEM of osteoblasts from the ovx group (×6700 magnification). TEM, transmission electron microscopy

the osteoblasts from the ovx group were lower than those in the sham group at the same time points (Figure 8).

Immunohistochemistry staining of UCP2

The UCP2 immunohistochemical staining of osteoblasts was observed as a yellow color that was concentrated in the cytoplasm of both groups; however, the signal in the osteoblasts from the sham group (Figure 9a) was higher than those from the ovx group (Figure 9b).

ATP quantification in osteoblasts

ATP concentrations of osteoblasts four and 12 weeks postsurgery were measured (Figure 10). The ATP concentrations of cells from the ovx groups were significantly higher than cells from the sham groups at four and 12 weeks postsurgery ($P < 0.05$). The ATP concentration was the highest in cells from the ovx group at 12 weeks postsurgery and lowest in cells from the sham group at the same time point.

ROS quantification in osteoblasts

Non-fluorescent DCFH can be oxidized by intracellular ROS to generate a fluorescent DCF, and therefore detection of DCF fluorescence can reflect the level of intracellular ROS. Four types of osteoblasts from the ovx and sham groups at four or 12 weeks postsurgery were detected using this method (Figure 11). There was a significant increase in

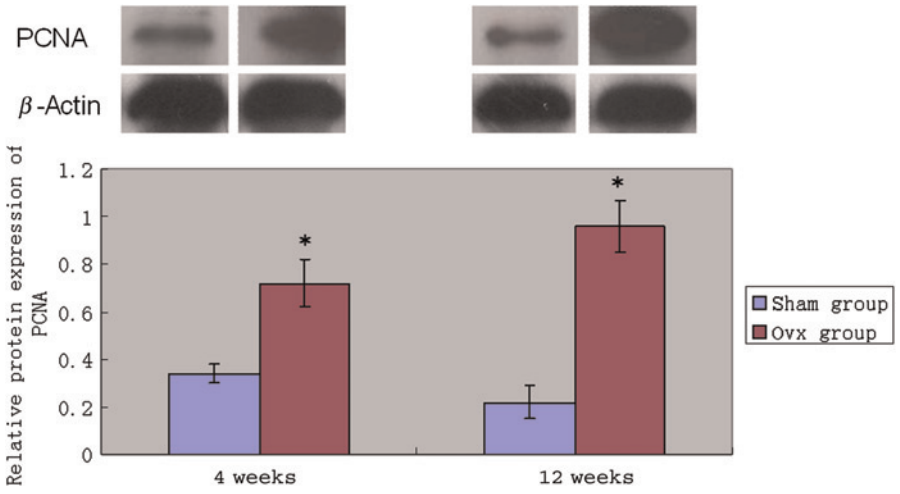

Figure 7 PCNA protein expression in the ovx and sham groups at different periods. $^{*}P < 0.05$ comparing the ovx and sham groups at the same time point. PCNA, proliferating cell nuclear antigen. (A color version of this figure is available in the online journal)

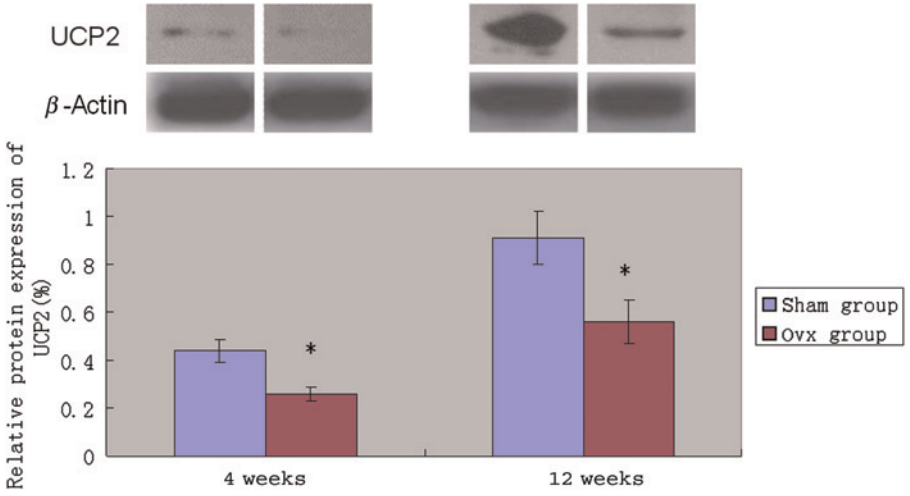

Figure 8 UCP2 protein expression in the ovx and sham groups at different time periods. $^{*}P < 0.05$ comparing the ovx and sham groups at the same time point. UCP2, uncoupling protein 2. (A color version of this figure is available in the online journal)

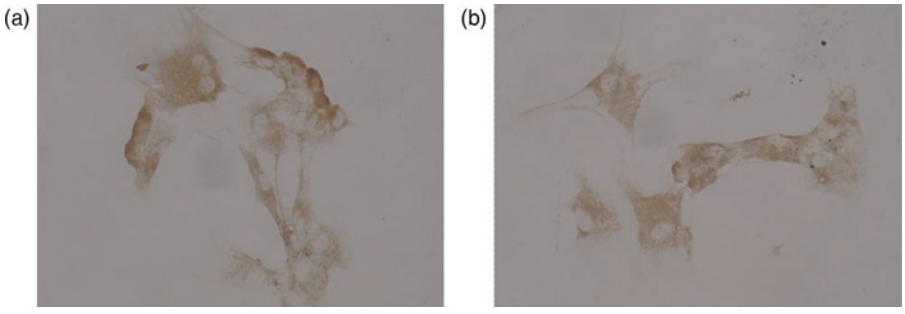

Figure 9 UCP2 immunohistochemical staining of osteoblasts: (a) UCP2 immunohistochemical staining from the sham group and (b) UCP2 immunohistochemical staining from the ovx group. UCP2, uncoupling protein 2A. (A color version of this figure is available in the online journal)

ROS concentrations of cells from the ovx group compared with the sham group ($P < 0.05$). In addition, osteoblasts from cells of the ovx group at 12 weeks postsurgery had the highest ROS concentrations, whereas osteoblasts from the sham group at four weeks postsurgery has the lowest.

Discussion

The surgical removal of rat ovaries is well recognized and accepted as a method for generating an osteoporotic animal model.[14] Some researchers believe that there is a significant correlation between the mineral density of the

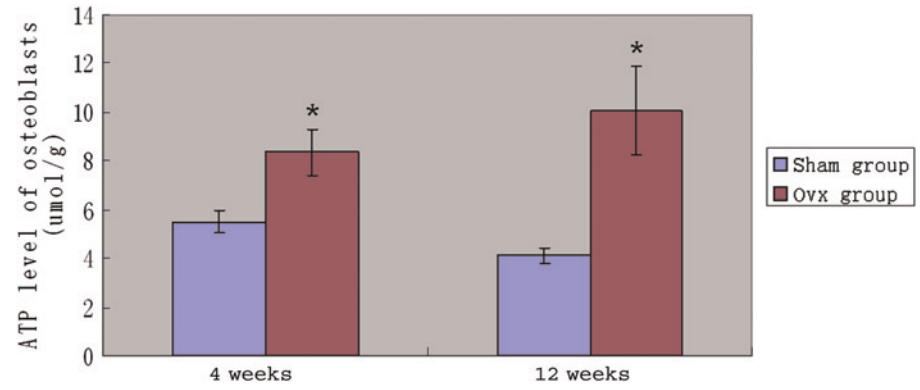

Figure 10 Differences in ATP production of osteoblasts between the ovx and sham groups at the same time point. (A color version of this figure is available in the online journal)

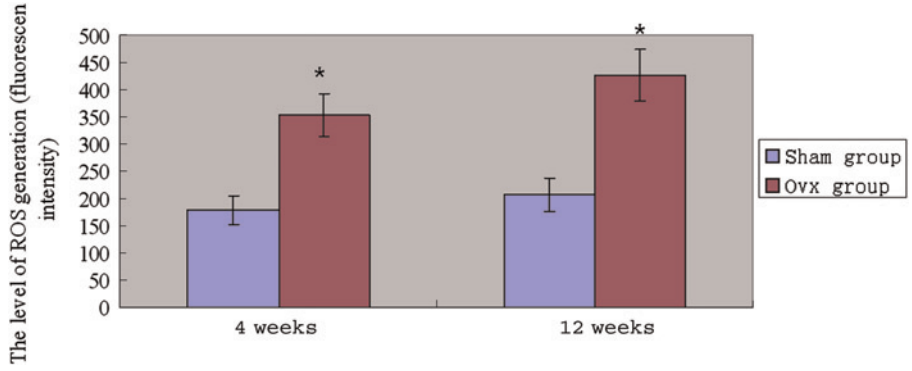

Figure 11 The level of reactive oxygen species (ROS) generation from osteoblasts of the ovx and sham groups. (A color version of this figure is available in the online journal)

mandibular bone and other bones in the body, so the mandibular BMD can be measured as a precursor to osteoporosis.[15,16] In this study, the lumbar spine and femur BMD in the ovx group decreased compared with the sham group at four weeks after the surgery, while the mandibular bone mineral density had an obvious increase. At 12 and 20 weeks after the operation, the mandibular BMD of the ovx group had a decreasing trend compared with the sham group. These results revealed that different parts of the osteoporotic body have different reactions to BMD. In addition, the decrease of BMD in different bone types of the body was not the same. The mandibular biopsy showed that at four weeks after the operation, the spongy bone at the root tip was sparse, even though the mandibular BMD increased. At 12 and 20 weeks after the operation, the sparseness of the trabecular bone was more obvious.

The masticatory functional and mechanical demands on the structural adaptation of the alveolar bone have an influence on BMD and bone microstructure parameters of the alveolar bone.[17] When measuring the BMD of the mandible, a lateral measurement can avoid the interference of other maxillofacial structures. However, because of too little bone and more cortical bone in the mandible, the decrease in BMD could not be measured during the early osteoporotic period.

Many studies hypothesized that the excessive absorption of osteoclasts was an important cause of osteoporosis.[18] Recent studies have found that osteoprotegerin (OPG), receptor activator of NF-κB ligand (RANKL), bone morphogenetic protein, matrix metalloproteinase and other cytokines expressed in osteoblasts link osteoblasts and osteoclasts together,[19–21] which indicates that osteoblasts play a more important role in osteoporosis than osteoclasts. Therefore, additional studies of osteoblasts may provide a deeper insight into the mechanisms of osteoporosis. Currently, there are several osteoblast-like cell lines that have been derived from tumor tissue or gene transfer methods, which have shown good stability and purity. However, osteoblast-like cell lines have undergone changes that may not adequately represent the normal physiological function, and their true representation of osteoblasts may be limited.[22] Importantly, primary cultures of osteoblasts from osteoporotic rats more accurately depict the *in vivo* situation than cell lines. Since osteoblasts from osteoporotic human bone have confounding factors, such as the patient's age, genetics, race and diet, the osteoporotic animal model provides a rich source of osteoblasts. Moreover, osteoblasts obtained from different sources can affect the biological characteristics of the cells.[23–25] Therefore, the successful culture of osteoblasts obtained from the mandible of osteoporotic rats in this study is an important breakthrough for experimental studies in oral medicine. The *in vitro* culture of osteoblasts not only eliminates the impact of complex factors within the body, but it also provides a source of the same seed cells.

The osteoblasts from the ovx group exhibited faster growth, earlier attachment and fewer dead cells at four and 12 weeks postsurgery compared with cells from the sham group. At 20 weeks, cells from both the ovx and sham groups grew slowly, did not passage smoothly and even died compared with cells at four or 12 weeks postsurgery. This may have been due to the age of the cells, since 32-week-old rats exhibit signs of aging based on published studies.[26,27] Osteoblasts from rats four and 12 weeks postsurgery were used for subsequent studies since a large number of cells were needed for proliferation, differentiation and related protein analyses. ATP provides energy for the growth, repair and physical activity of osteoblasts, and has been described as the energy currency of the cell.[28] The higher growth and passage ability of osteoblasts from the ovx group may be closely related to higher energy metabolism, especially in the generation of ATP, and therefore an analysis of ATP in osteoblasts from an osteoporotic model may help explain the abnormal performance of osteoblasts. We found that the proliferation and differentiation ability of cells from the ovx groups increased compared with the sham groups, as determined with the MTT, ALP activity and osteocalcin (OC) release assays. TEM also verified the higher proliferation and differentiation ability of osteoblasts from the ovx group, which had more heterochromatin and mitochondria, but fewer folds, lysosomes, peroxisomes and nucleoli.

The development of methods for culturing osteoblasts *in vitro* has enhanced experimental studies and allowed researchers to investigate osteoblast metabolism in healthy tissue and in various different bone diseases. A greater knowledge of cultures from pathological bone tissue-derived osteoblasts may be helpful in performing *in vitro* experiments, since this kind of approach better reflects the conditions of clinically relevant diseases. In ovariectomized rats at four weeks (early osteoporosis), the proliferation and differentiation ability of the osteoblasts increased significantly. This suggested that the osteoblast changes occurred earlier than BMD, so some characteristics of osteoblasts may be important for the prevention and treatment of osteoporosis. In the absence of a body substance, the ability to make body precision adjustments provided long-term compensation. In other words, the removal of the ovaries reduced the estrogen concentrations, which created a need for the enhancement of osteoblast function in order to compensate for the effects of the decrease in estrogen. This compensatory function of the body may be an important method for treating chronic diseases. In most cases, when the loss of an important factor is not properly compensated, life-sustaining activities are prioritized to maintain important regulatory mechanisms. In addition, the more active *in vitro* growth of osteoblasts from the ovx group may be due to an increase in factors, such as serum factors and receptors on the osteoblasts, which disturb the balance between osteoblasts and osteoclasts.[29,30] The function of osteoclasts is overactivated by certain factors secreted by osteoblasts. The application of OPG has been shown to be a possible method for preventing and treating osteoporosis.[31,32] Therefore, the search for differences between normal osteoblasts and osteoblasts from the osteoporotic body may identify promising treatment options for osteoporosis, and a preliminary assessment of these mechanisms was made in this study. A previous study had shown that osteoblastic cells derived from trabecular bone explants of osteoporotic subjects (OP cells) exhibited an altered ALP response to 1,25-dihydroxyvitamin D3 (1,25(OH)2D3) compared with control (CON) cells. In addition, dexamethasone was shown to amplify the differences between OP and CON cells and confirmed the presence of intrinsic osteoblastic abnormalities in patients with osteoporosis that persisted in culture.[33] Early adhesion-mediated events, such as cell adhesion, attachment, and focal adhesion kinase signaling through phosphotyrosine may be altered in osteoporotic osteoblasts.[24] Under baseline conditions, human normal and osteoporotic bone cells showed some differences *in vitro* in proliferation (MTT test), procollagen I carboxyterminal propeptide and OC assays, as well as interleukin-6 levels. Importantly, the current findings should also be considered with the findings from *in vitro* cultures derived from the human bone.[34]

PCNA was originally identified as an antigen that is expressed in the nuclei of cells during the DNA synthesis phase of the cell cycle.[35] The level of expression is closely related to cell proliferation activity.[36] In this study, the proliferation of osteoblasts appeared to increase, which was consistent with the expression of PCNA. In addition, the increase in proliferation and differentiation was confirmed by the TEM results. The increase in the number of mitochondria in this study reflected the active state of the osteoblasts. The changes in the number of mitochondria indicated the pathological changes of osteoblasts for energy production and use. Mitochondria are the power plant of cells and provide the energy for cell proliferation and differentiation. Some researchers have found a relationship between osteoporosis and the cytochrome *c* of mitochondria, and cytochrome *c* plays a role in the apoptosis of osteoblasts.[37–39] In addition, other proteins of the mitochondria may also be involved in cell energy metabolism. UCP2 is a proton transporter on the mitochondrial inner membrane and is widely found in brown adipose tissue, white adipose tissue, skeletal muscle, pancreatic β-cells, liver, heart, spleen, kidney, brain, lymphocytes, placenta and intestinal cells.[40–45] UCP2 was shown to provide protective effects by transferring the superoxide anion from the substrate to the space inside and outside of the mitochondrial membrane.[46,47] UCP2 expression can be induced[48] and regulated by many factors, such as 1,25(OH)2D3, thyroid hormone, growth hormone, leptin, norepinephrine, nucleation peroxidase, peroxisome proliferator-activated receptor γ, diet, exercise and ultrasound stimulation.[49–53] In addition, the degree of UCP2 expression is closely related to several physiological and pathological processes. The UCP2 expression in white adipose tissue of ovx rats has been shown to be reduced, which was related to the reduction of estrogen.[54] Moreover, UCP2 is an important intracellular protein that inhibits the production of ROS.[55–57] The down-regulation of ROS production through the activation of UCP2 may provide a unique strategy for the prevention and treatment of chronic diseases, including osteoporosis, since the protein is widely expressed in numerous mammalian tissues, yet in

minute amounts. Fatokun *et al*.[58] reported that ROS could influence MC3T3-E1 osteoblast-like cells and was related to conditions such as osteoporosis. On the other hand, UCP2 can mediate mitochondrial proton leak, which can dissipate the protons originally used for ATP synthesis, which suggests that UCP2 activation may lead to a decline in ATP synthesis. ATP is involved in a variety of enzymatic reactions *in vivo* to maintain normal life activities and is an indicator of living cell metabolism. Therefore, ATP content can be used as a quantitative indicator of cell proliferation and cytotoxicity.

In this study, immunohistochemistry and Western blot analysis showed that UCP2 was expressed in osteoblasts, and the results suggest that the UCP2 expression levels in the osteoblasts from osteoporotic rats were lower than in the sham group. However, the concentrations of ATP and ROS were significantly higher in cells of the ovx group than the sham group. These data may indicate the relationship between UCP2, ATP and ROS. It is possible that due to the decreased UCP2 expression, which reduced mitochondrial proton leak, ATP production increased and provided energy for the osteoblasts, which increased the proliferation and differentiation. Concurrently, excessive protons for osteoblasts may have produced certain toxic effects that affected osteoblasts, which enhanced the inflammatory response, possibly through increased expression of ROS and superoxide anions. These effects caused a pathological state in the osteoblasts. Therefore, studies of UCP2 may provide an approach for the prevention and treatment of osteoporosis.

The results of this study suggest that there are differences in cell ultrastructure, proliferation, differentiation, ATP and ROS concentrations, and PCNA and UCP2 protein expression levels between the osteoblasts from the mandibles of rats of the ovx and sham groups. In addition, the *in vitro* culture method of osteoporotic osteoblasts from mandibles described in this study may provide a way of studying osteoporosis in oral medicine.

Author contributions: G-XZ and H-CL designed the experiment; S-JY, G-XZ and H-CL wrote the paper; and S-JY, L-LE and D-SW performed the experiments. None of the authors have conflicts of interests and all authors approved the submission.

REFERENCES

1 Heaney RP. Remodeling and skeletal fragility. *Osteoporos Int* 2003;**14**(Suppl 5):S12–5
2 Johnell O, Kanis JA. An estimate of the worldwide prevalence and disability associated with osteoporotic fractures. *Osteoporos Int* 2006;**17**:1726–33
3 Li SL, Gao H, Zhang KH. Effects of epimedium on proliferation, function and apoptosis of mouse osteoblasts *in vitro*. *Beijing Da Xue Xue Bao* 2008;**40**:43–6
4 Kim CH, Kim YH, Kim YK, Kang BS, Lee TK, Moon SH, Park YG. IL-1beta induces and TGF-beta reduces vitamin D3-induced bone resorption in mouse calvarial bone cells. *Immunol Invest* 2003;**32**:171–86
5 Poulsen RC, Moughan PJ, Kruger MC. Long-chain polyunsaturated fatty acids and the regulation of bone metabolism. *Exp Biol Med (Maywood)* 2007;**232**:1275–88
6 Choi EM, Lee YS. Mitochondrial defects and cytotoxicity by antimycin A on cultured osteoblastic MC3T3-E1 cells. *Food Chem Toxicol* 2011;**49**:2459–63
7 Choi EM. Kaempferol protects MC3T3-E1 cells through antioxidant effect and regulation of mitochondrial function. *Food Chem Toxicol* 2011;**49**:1800–5
8 Katz S, Ayala V, Santillán G, Boland R. Activation of the PI3K/Akt signaling pathway through $P2Y_2$ receptors by extracellular ATP is involved in osteoblastic cell proliferation. *Arch Biochem Biophys* 2011;**513**:144–52
9 Genetos DC, Geist DJ, Liu D, Donahue HJ, Duncan RL. Fluid shear-induced ATP secretion mediates prostaglandin release in MC3T3-E1 osteoblasts. *Bone* 2005;**20**:41–9
10 Cline GW. Fuel-stimulated insulin secretion depends upon mitochondria activation and the integration of mitochondrial and cytosolic substrate cycles. *Diabetes Metab J* 2011;**35**:458–65
11 Robson-Doucette CA, Sultan S, Allister EM, Wikstrom JD, Koshkin V, Bhatacharjee A, Prentice KJ, Sereda SB, Shirihai OS, Wheeler MB. Beta-cell uncoupling protein 2 regulates reactive oxygen species production, which influences both insulin and glucagon secretion. *Diabetes* 2011;**60**:2710–9
12 Goldhahn J, Neuhoff D, Schaeren S, Steiner B, Linke B, Aebi M, Schneider E. Osseointegration of hollow cylinder based spinal implants in normal and osteoporotic vertebrae: a sheep study. *Arch Orthop Trauma Surg* 2006;**126**:554–61
13 Marcu F, Bogdan F, Mutiu G, Lazar L. The histopathological study of osteoporosis. *Rom J Morphol Embryol* 2011;**52**(Suppl):321–5
14 Thorndike EA, Turner AS. In search of an animal model for postmenopausal diseases. *Front Biosci* 1998;**3**:c17–26
15 Kuroda S, Mukohyama H, Kondo H, Aoki K, Ohya K, Ohyama T, Kasugai S. Bone mineral density of the mandible in ovariectomized rats: analyses using dual energy X-ray absorptiometry and peripheral quantitative computed tomography. *Oral Dis* 2003;**9**:24–8
16 Horner K, Devlin H, Alsop CW, Hodgkinson IM, Adams JE. Mandibular bone mineral density as a predictor of skeletal osteoporosis. *Br J Radiol* 1996;**69**:1019–25
17 Mavropoulos A, Kiliaridis S, Bresin A, Ammann P. Effect of different masticatory functional and mechanical demands on the structural adaptation of the mandibular alveolar bone in young growing rats. *Bone* 2004;**35**:191–7
18 Kowada T, Kikuta J, Kubo A, Ishii M, Maeda H, Mizukami S, Kikuchi K. *In vivo* fluorescence imaging of bone-resorbing osteoclasts. *J Am Chem Soc* 2011;133:17772–6
19 Silva I, Branco JC. Rank/Rankl/opg: literature review. *Acta Reumatol Port* 2011;**36**:209–18
20 Chen PY, Sun JS, Tsuang YH, Chen MH, Weng PW, Lin FH. Simvastatin promotes osteoblast viability and differentiation via Ras/Smad/Erk/BMP-2 signaling pathway. *Nutr Res* 2010;**30**:191–9
21 Li J, Liao EY, Dai RC, Wei QY, Luo XH. Effects of 17 beta-estradiol on the expression of interstitial collagenases-8 and -13 (MMP-8 and MMP-13) and tissue inhibitor of metalloproteinase-1 (TIMP-1) in ovariectomized rat osteoblastic cells. *J Mol Histol* 2004;**35**:723–31
22 Cenni E, Ciapetti G, Granchi D, Arciola CR, Savarino L, Stea S, Montanaro L, Pizzoferrato A. Established cell lines and primary cultures in testing medical devices *in vitro*. *Toxicol In Vitro* 1999;13:801–10
23 Marie PJ, Hott M, Launay JM, Graulet AM, Gueris J. *In vitro* production of cytokines by bone surface-derived osteoblastic cells in normal and osteoporotic postmenopausal women: relationship with cell proliferation. *J Clin Endocrinol Metab* 1993;77:824–30
24 Perinpanayagam H, Zaharias R, Stanford C, Brand R, Keller J, Schneider G. Early cell adhesion events differ between osteoporotic and non-osteoporotic osteoblasts. *J Orthop Res* 2001;**19**:993–1000
25 Komm BS, Terpening CM, Benz DJ, Graeme KA, Gallegos A, Korc M, Greene GL, O'Malley BW, Haussler MR. Estrogen binding, receptor mRNA, and biologic response in osteoblast-like osteosarcoma cells. *Science* 1988;**241**:81–4
26 Kiss A, Delattre AM, Pereira SI, Carolino RG, Szawka RE, Anselmo-Franci JA, Zanata SM, Ferraz AC. 17β-Estradiol replacement in young, adult and middle-aged female ovariectomized rats promotes improvement of spatial reference memory and an antidepressant effect and alters monoamines and BDNF levels in memory- and depression-related brain areas. *Behav Brain Res* 2011;**227**:100–8

27 Erben RG, Lausmann K, Roschger P, Schüler C, Skalicky M, Klaushofer K, Windisch W. Long-term marginal zinc supply is not detrimental to the skeleton of aged female rats. *J Nutr* 2009;**139**:703–9
28 Gallagher JA. ATP P2 receptors and regulation of bone effector cells. *J Musculoskelet Neuronal Interact* 2004;**4**:125–7
29 Yokose S, Ishizuya T, Ikeda T, Nakamura T, Tsurukami H, Kawasaki K, Suda T, Yoshiki S, Yamaguchi A. An estrogen deficiency caused by ovariectomy increases plasma levels of systemic factors that stimulate proliferation and differentiation of osteoblasts in rats. *Endocrinology* 1996;**137**:469–78
30 Modrowski D, Miravet L, Feuga M, Marie PJ. Increased proliferation of osteoblast precursor cells in estrogen-deficient rats. *Am J Physiol* 1993;**264**(Part 1):E190–6
31 Zhao Y, Li J, Liu Y, Yu KQ, Zhang J, Chen XG. Gu Ling Pian, a traditional Chinese medicine, regulates function and OPG/RANKL synthesis of osteoblasts via the p38 MAPK pathway. *J Pharm Pharmacol* 2007;**59**:1167–73
32 Schindeler A, Little DG. Bisphosphonate action: revelations and deceptions from *in vitro* studies. *J Pharm Sci* 2007;**96**:1872–8
33 Rao LG, Murray TM, Wylie JN, McBroom RJ, Sutherland MK. Long-term culture in dexamethasone unmasks an abnormal phenotype in osteoblasts isolated from osteoporotic subjects. *J Endocrinol Invest* 2005;**28**:919–27
34 Torricelli P, Fini M, Giavaresi G, Giardino R. Human osteoblast cultures from osteoporotic and healthy bone: biochemical markers and cytokine expression in basal conditions and in response to 1,25(OH)2D3. *Artif Cells Blood Substit Immobil Biotechnol* 2002;**30**:219–27
35 Leonardi E, Girlando S, Serio G, Mauri FA, Perrone G, Scampini S, Dalla Palma P, Barbareschi M. PCNA and Ki67 expression in breast carcinoma: correlations with clinical and biological variables. *J Clin Pathol* 1992;**45**:416–9
36 Abshagen K, Eipel C, Menger MD, Vollmar B. Comprehensive analysis of the regenerating mouse liver: an *in vivo* fluorescence microscopic and immunohistological study. *J Surg Res* 2006;**134**:354–62
37 Tanaka S, Haji M, Takayanagi R, Sugioka Y, Nawata H. 1,25-Dihydroxyvitamin D3 enhances the enzymatic activity and expression of the messenger ribonucleic acid for aromatase cytochrome P450 synergistically with dexamethasone depending on the vitamin D receptor level in cultured human osteoblasts. *Endocrinology* 1996;**137**:1860–9
38 Takayanagi R, Goto K, Suzuki S, Tanaka S, Shimoda S, Nawata H. Dehydroepiandrosterone (DHEA) as a possible source for estrogen formation in bone cells: correlation between bone mineral density and serum DHEA-sulfate concentration in postmenopausal women, and the presence of aromatase to be enhanced by 1,25-dihydroxyvitamin D3 in human osteoblasts. *Mech Ageing Dev* 2002;**123**:1107–14
39 Kim DJ, Koh JM, Lee O, Kim NJ, Lee YS, Kim YS, Park JY, Lee KU, Kim GS. Homocysteine enhances apoptosis in human bone marrow stromal cells. *Bone* 2006;**39**:582–90
40 Rey B, Sibille B, Romestaing C, Belouze M, Letexier D, Servais S, Barré H, Duchamp C, Voituron Y. Reptilian uncoupling protein: functionality and expression in sub-zero temperatures. *J Exp Biol* 2008;**211**(Part 9):1456–62
41 Ren D, Jin J, Li X, Zeng G. Change of chart genes expression in small intestines of mouse induced by electromagnetic pulse irradiation. *Wei Sheng Yan Jiu* 2008;**37**:22–4
42 Fleury C, Neverova M, Collins S, Raimbault S, Champigny O, Levi-Meyrueis C, Bouillaud F, Seldin MF, Surwit RS, Ricquier D, Warden CH. Uncoupling protein-2: a novel gene linked to obesity and hyperinsulinemia. *Nat Genet* 1997;**15**:269–72
43 Pecqueur C, Alves-Guerra MC, Gelly C, Levi-Meyrueis C, Couplan E, Collins S, Ricquier D, Bouillaud F, Miroux B. Uncoupling protein 2, *in vivo* distribution, induction upon oxidative stress, and evidence for translational regulation. *J Biol Chem* 2001;**276**:8705–12
44 Zhang CY, Baffy G, Perret P, Krauss S, Peroni O, Grujic D, Hagen T, Vidal-Puig AJ, Boss O, Kim YB, Zheng XX, Wheeler MB, Shulman GI, Chan CB, Lowell BB. Uncoupling protein-2 negatively regulates insulin secretion and is a major link between obesity, beta cell dysfunction, and type 2 diabetes. *Cell* 2001;**105**:745–55
45 Medvedev AV, Robidoux J, Bai X, Cao W, Floering LM, Daniel KW, Collins S. Regulation of the uncoupling protein-2 gene in INS-1 beta-cells by oleic acid. *J Biol Chem* 2002;**277**:42639–44
46 Echtay KS, Winkler E, Frischmuth K, Klingenberg M. Uncoupling proteins 2 and 3 are highly active H(+) transporters and highly nucleotide sensitive when activated by coenzyme Q (ubiquinone). *Proc Natl Acad Sci USA* 2001;**98**:1416–21
47 Otaegui D, Saenz A, Ruiz-Martinez J, Olaskoaga J, Lopez de Munain A. UCP2 and mitochondrial haplogroups as a multiple sclerosis risk factor. *Mult Scler* 2007;**13**:454–8
48 Kimura K, Jung BD, Kanehira K, Irie Y, Canas X, Saito M. Induction of uncoupling protein (UCP) 2 in primary cultured hepatocytes. *FEBS Lett* 1999;**457**:75–9
49 Sun X, Zemel MB. Role of uncoupling protein 2 (UCP2) expression and 1alpha, 25-dihydroxyvitamin D3 in modulating adipocyte apoptosis. *FASEB J* 2004;**18**:1430–2
50 Collin A, Cassy S, Buyse J, Decuypere E, Damon M. Potential involvement of mammalian and avian uncoupling proteins in the thermogenic effect of thyroid hormones. *Domest Anim Endocrinol* 2005;**29**:78–87
51 Scarpace PJ, Nicolson M, Matheny M. UCP2, UCP3 and leptin gene expression: modulation by food restriction and leptin. *J Endocrinol* 1998;**159**:349–57
52 Kato H, Ohue M, Kato K, Nomura A, Toyosawa K, Furutani Y, Kimura S, Kadowaki T. Mechanism of amelioration of insulin resistance by beta3-adrenoceptor agonist AJ-9677 in the KK-Ay/Ta diabetic obese mouse model. *Diabetes* 2001;**50**:113–22
53 Boss O, Hagen T, Lowell BB. Uncoupling proteins 2 and 3: potential regulators of mitochondrial energy metabolism. *Diabetes* 2000;**49**:143–56
54 Pedersen SB, Bruun JM, Kristensen K, Richelsen B. Regulation of UCP1, UCP2, and UCP3 mRNA expression in brown adipose tissue, white adipose tissue, and skeletal muscle in rats by estrogen. *Biochem Biophys Res Commun* 2001;**288**:191–7
55 Cho P, Schneider GB, Krizan K, Keller JC. Examination of the bone-implant interface in experimentally induced osteoporotic bone. *Implant Dent* 2004;**13**:79–87
56 Kizaki T, Suzuki K, Hitomi Y, Taniguchi N, Saitoh D, Watanabe K, Onoé K, Day NK, Good RA, Ohno H. Uncoupling protein 2 plays an important role in nitric oxide production of lipopolysaccharide-stimulated macrophages. *Proc Natl Acad Sci USA* 2002;**99**:9392–7
57 Blanc J, Alves-Guerra MC, Esposito B, Rousset S, Gourdy P, Ricquier D, Tedgui A, Miroux B, Mallat Z. Protective role of uncoupling protein 2 in atherosclerosis. *Circulation* 2003;**107**:388–90
58 Fatokun AA, Stone TW, Smith RA. Responses of differentiated MC3T3-E1 osteoblast-like cells to reactive oxygen species. *Eur J Pharmacol* 2008;**587**:35–41

(Received June 17, 2011, Accepted December 15, 2011)